Robust Numerical Analysis of Wound Core Distribution Transformers

Themistoklis D. Kefalas and Antonios G. Kladas, *Member, IEEE*
Faculty of Electrical and Computer Engineering, National Technical University of Athens
thkefala@central.ntua.gr

***Abstract*-In this paper a robust three-dimensional (3D) finite element (FE) anisotropy model is introduced based on a particular scalar potential formulation. The specific 3D FE model is suitable for the accurate evaluation of the peak flux density distribution and no load loss of one-phase and three-phase wound core distribution transformers. The accuracy of the proposed 3D FE anisotropy model is validated by local flux density and no load loss measurements.**

I. INTRODUCTION

Accurate flux density distribution and no load loss evaluation of wound core distribution transformers present significant difficulties and analytical relationships usually do not suffice [1]. A satisfactory estimation can be achieved however, by using field analysis numerical techniques in conjunction with the detailed modeling of the core's magnetic material properties [2].

In order to compute accurately the wound core's flux density distribution, each individual steel sheet and the varnish between successive sheets must be modeled. This approach was followed recently for the simulation of toroidal wound cores consisting of a small number of steel sheets [3]. The disadvantage of the aforementioned approach is its extremely high computational cost that limits the effectiveness of the method only to two-dimensional (2D) applications [3], despite the recent advancements in computing. Furthermore, typical wound cores, used for the construction of distribution transformers, consist of hundreds grain-oriented steel sheets and even the 2D field analysis is practically impossible due to the inherent large mesh size required to represent the laminated core.

In the present paper the accurate representation of the wound core with a low computational cost is achieved by considering the iron-laminated material as homogeneous media and by developing an elliptic anisotropy model specifically formulated for wound cores [4], [5]. The elliptic anisotropy model takes into account the directional dependence of the B-H characteristic due to the iron laminations and the grain orientation of the grain-oriented electrical steel used for the construction of the wound cores.

In order to reduce further the computational requirements a particular reduced scalar potential formulation, necessitating no prior source field calculation [6], is adopted enabling the three-dimensional (3D) magnetostatic field analysis of wound core distribution transformers.

II. 3D FE FORMULATION

The solution of 3D magnetostatic problems by the finite element (FE) method based on the magnetic vector potential (MVP) is quite laborious as there are three unknown components to be determined at each node of the FE mesh. Furthermore the solution has be found to be erroneous when the normal component of the MVP is significant at the interface between regions of different permeability, e.g. at the interface between iron and air [6].

On the other hand magnetic scalar potential (MSP) based FE formulations are advantageous in terms of computational effort, as there is only one degree of freedom to be evaluated for every node of the FE mesh. Despite this obvious advantage, many problems arise with the use of the MSP like inherent difficulties in handling 3D volume current distributions, cancellation errors in the iron domain, difficulties in modeling multiply connected iron regions, and multiply valued potentials [6]. A number of scalar potential formulations have been developed to address some of the latter problems like the difference potential (DP) and the total scalar potential (TP) formulation. Those early formulations have been united and extended by the general potential (GP) formulation [7], [8]. According to the GP formulation the magnetic field intensity $\mathbf{H}$ is sought in the following form

$$\mathbf{H} = \mathbf{H}_g + \nabla \Phi_g \tag{1}$$

where $\mathbf{H}_g$ is an initial guess magnetic field and Φ_g is the general potential. If $\mathbf{H}_g$ satisfies Ampere's law and its absolute value is much larger than that of $\nabla \Phi_g$ then the solution of the problem can be found according to

$$\nabla \cdot \left(\boldsymbol{\mu} \cdot \left(\mathbf{H}_g + \nabla \Phi_g \right) \right) = 0. \tag{2}$$

What remains is the evaluation of a suitable guess field $\mathbf{H}_g$ with the following three-step scheme proposed in [7], [8].

1. First compute the guess magnetic field $\mathbf{H}_{gi}$, in the iron domain by satisfying the following conditions.

$$\nabla \cdot \left(\boldsymbol{\mu} \cdot \mathbf{H}_{gi} \right) = 0 \tag{3}$$

$$\mathbf{n} \cdot \left(\boldsymbol{\mu} \cdot \mathbf{H}_{gi} \right) = 0 \tag{4}$$

978-1-4244-1736-0/08/$25.00 ©2008 IEEE

2. Then compute the guess magnetic field $\mathbf{H}_{go}$, in the air domain by satisfying the following conditions.

$$\nabla \cdot \left(\boldsymbol{\mu} \cdot \mathbf{H}_{go}\right) = 0 \tag{5}$$

$$\nabla \times \left(\mathbf{H}_{go}\right) = \mathbf{J}_{o} \tag{6}$$

$$\mathbf{n} \times \left(\mathbf{H}_{gi} - \mathbf{H}_{go}\right) = 0 \tag{7}$$

3. Calculate the general potential Φ_g over the whole domain by satisfying (2).

Even though the GP formulation covers successfully most of the practical engineering problems there are two disadvantages. The first one is the complexity of the GP formulation since a three-step procedure is required to obtain the solution. The second one is that for a nonlinear analysis several iterations are required during the execution not only of the third step but also of the first step. These disadvantages lead to increasing computational effort and time.

In this paper, it is proposed to use a particular scalar potential formulation necessitating no prior source field calculation, presented in [6]. According to this formulation $\mathbf{H}$ is partitioned as follows

$$\mathbf{H} = \mathbf{K} - \nabla \Phi \tag{8}$$

where Φ is a scalar potential extended all over the solution domain and $\mathbf{K}$ is a fictitious field distribution that satisfies the following three conditions.

1. $\mathbf{K}$ is confined in a simply connected subdomain comprising the coil region.

2. In the coil domain and outside the coil domain $\mathbf{K}$ satisfies (9) and (10) respectively.

$$\nabla \times \mathbf{K} = \mathbf{J} \tag{9}$$

$$\nabla \times \mathbf{K} = \mathbf{0} \tag{10}$$

3. Finally $\mathbf{K}$ is perpendicular on the boundary of the subdomain comprising the coil region.

The above conditions constitute a minimum enabling to simulate the coil. The distribution of $\mathbf{K}$ is easily determined analytically or numerically by the conductors shape with little computational effort [6]. The problem's solution is obtained by discretizing (11) that ensures the total's field solenoidality.

$$\nabla \cdot \left(\boldsymbol{\mu} \cdot \left(\mathbf{K} - \nabla \Phi\right)\right) = 0 \tag{11}$$

The previous formulation does not suffer from cancellation errors, it satisfies Ampere's law, and consequently it is applicable to multiply connected iron regions. Simplicity and computational efficiency are its main advantages in contrast with the GP formulation.

III. Elliptic Anisotropy Model

By considering the iron-laminated material as homogeneous and anisotropic media at the level of finite elements an accurate representation of the wound core is achieved. An elliptic anisotropy model is best suited for the wound core transformer in contrast with the stack core transformer [9]. The specific model is based on the assumption that the magnetic field intensity has an elliptic trajectory for the modulus of the flux density constant [4], [5].

A simplified graphical interpretation of this assumption is given in Figs. 1, 2. Fig. 1 depicts B - H characteristics of the electrical steel for various angles to the rolling direction. For a constant flux density the magnetic field intensity tends to increase as the angle to the rolling direction increases. By projecting the values of the magnetic field intensity for different directions of the field to the H_p - H_q plane, where p and q is the direction tangential and normal to the rolling direction respectively, a curve is formed as shown in Fig 2. This curve can be approximated by an ellipse and in the case of laminated wound cores this approximation leads to an error that rarely exceeds a few percentage points.

Therefore, if μ_p is the magnetic permeability tangential to the electrical steel rolling direction, μ_q is the permeability normal to the rolling direction, and r is the ratio of the ellipse p semi-axes to the ellipse q semi-axes then

$$\mu_q = r\mu_p, \quad 0 < r < 1. \tag{12}$$

Fig. 3 illustrates an ellipse in the H_p - H_q plane for an arbitrary value of flux density, where $H\left(0^o\right)$, $H\left(90^o\right)$ are the respective values of the magnetic field intensity tangential and normal to the rolling direction.

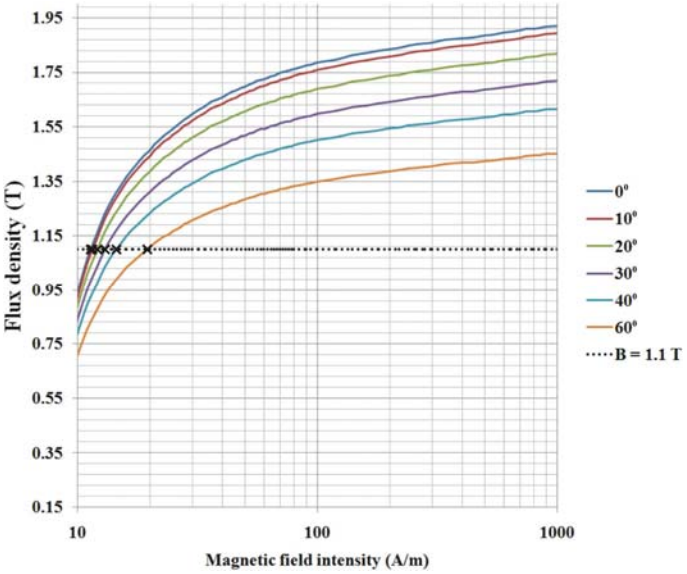

Fig. 1. *B-H* characteristics for various angles to the rolling direction.

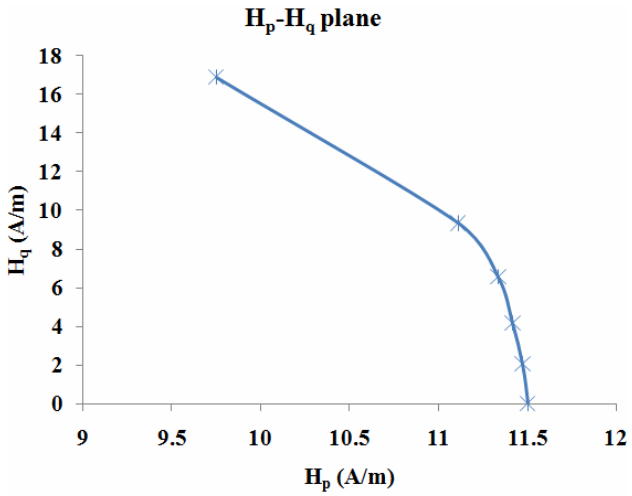

Fig. 2. Trajectory of the magnetic field intensity in the H_p-H_q plane.

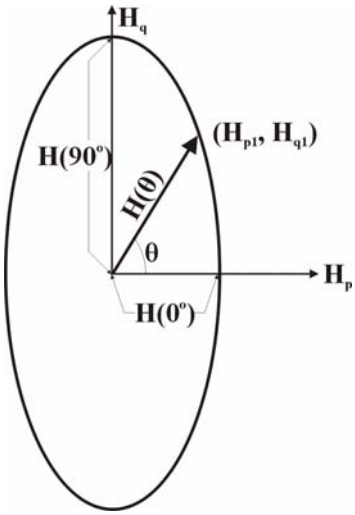

Fig. 3. Ellipse in the H_p-H_q plane.

The equation of the ellipse of Fig. 3 is given by (13) whereas the ratio of the ellipse semi-axes is given also by (14).

$$\frac{H_p^2}{H(0^o)^2}+\frac{H_q^2}{H(90^o)^2}=1 \tag{13}$$

$$r=\frac{H(0^o)}{H(90^o)} \tag{14}$$

Substituting (14) into (13) yields

$$H_p^2+r^2H_q^2=H(0^o)^2. \tag{15}$$

For an arbitrary angle θ to the rolling direction and from Fig. 3, it follows that the two components H_{p1}, H_{q1} of the magnetic field intensity are given by

$$H_{p1}=H\cos\theta,\quad H_{q1}=H\sin\theta. \tag{16}$$

The point (H_{p1}, H_{q1}) satisfies also the equation of the ellipse. So by substituting (16) into (15) it follows that

$$H(\theta)=\frac{H(0^o)}{\sqrt{1+(r^2-1)\sin^2\theta}}. \tag{17}$$

In order to determine the B-H characteristics of the air (varnish)-iron composite of the laminated wound core, one can express from magnetic circuit concepts the magnetic permeability tangential and normal to the rolling direction by (18) and (19) respectively

$$\mu_p=\mu_0\left[c_{sf}\mu_r+(1-c_{sf})\right] \tag{18}$$

$$\mu_q=\frac{\mu_r\mu_0}{\left[c_{sf}+(1-c_{sf})\mu_r\right]} \tag{19}$$

where μ_0 is the magnetic permeability of the air, μ_r is the relative magnetic permeability of the electrical steel obtained by the normal magnetization curve of the electrical steel and c_{sf} is the wound core's stacking factor. The magnetic permeability μ_z orthogonal to the p-q plane, shown in Fig. 4, is taken to be equal to the magnetic permeability along the rolling direction μ_p. Even though this assumption is not true it does not affect the flux density distribution evaluation of wound cores due to the symmetry of the problem.

The evaluation of the magnetic field intensity with the aforementioned elliptic anisotropy model is very simple and only the normal magnetization curve and the wound core stacking factor must be known. To sum up, the procedure for the calculation of the magnetic field intensity for an arbitrary flux density and angle to the rolling direction is the following.

Fig. 4. Typical wound core and p, q, z, directions.

1. For an arbitrary value of B calculate μ_r from the normal magnetization curve of the electrical steel.
2. Compute μ_p and μ_q using (18) and (19).
3. Calculate r from (12) and $H(0^o)$ from (20).

$$H(0^o) = B / \mu_p \tag{20}$$

4. Finally, for an arbitrary θ evaluate H using (17).

Due to the wound core's geometry shown in Fig. 4, the permeability tensor must be rotated to a different coordinate system in some of the areas of the 3D FE model. The permeability tensor $\boldsymbol{\mu}$ in the global coordinate system is given by (21), where $\mathbf{R}$ is the rotation matrix and $\boldsymbol{\mu}_F$ is the permeability tensor in the local coordinate system.

$$\boldsymbol{\mu} = \mathbf{R}^{-1} \boldsymbol{\mu}_F \mathbf{R} \tag{21}$$

The evaluation of the peak flux density distribution with the specific FE method is used in conjunction with the experimentally determined local specific core loss SCL, expressed as a function of the peak flux density and approximated by cubic splines, for the evaluation of the wound core no load loss. Fig. 5 shows the post processing algorithm used for the evaluation of the no load loss where SCL_i, B_i, P_i, V_i, are the specific core loss, peak flux density, no load loss and volume respectively of the i-th tetrahedron, d_{ms} is the magnetic steel's density, P_{NLL} is the no load loss and n is the number of tetrahedrons of the 3D FE mesh.

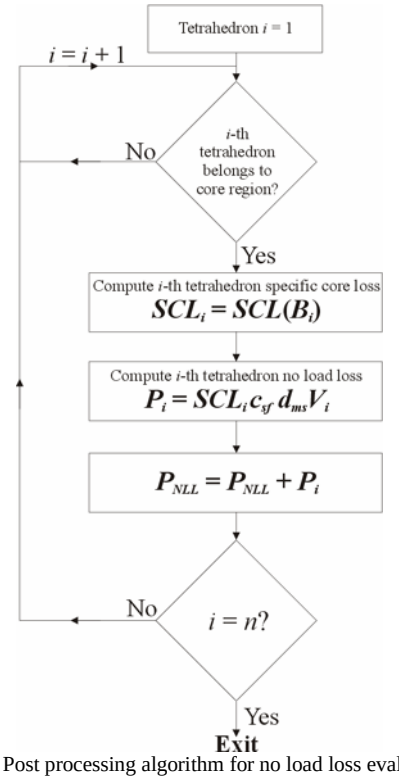

Fig. 5. Post processing algorithm for no load loss evaluation.

IV. Experimental Verification of the 3D FE Model

The 3D FE anisotropy model presented in Sections II and III was used for the numerical analysis of various one-phase, and three-phase wound core transformers. The computed no load loss value and peak flux density distribution were compared to the measured ones.

The experimental setup used for the local flux density and no load loss measurements of wound cores is illustrated in Fig. 6. It consists of a PC and a National Instruments (NI) 6143 data acquisition (DAQ) card (8 voltage differential inputs, 16 bit, 250 ksamples / s). The excitation coil terminals are connected to the input of the DAQ card via an active differential voltage probe (3 dB frequency of 18 MHz) and a current probe based on the Hall Effect (1 dB frequency of 150 kHz) is used for capturing the no load current, shown in Fig. 7. For the magnetization of the wound cores, a 23 turn excitation coil is supplied by a one-phase 230 V, 50 Hz source through a variable transformer. The no load loss was evaluated by the acquired voltage and current data with appropriate virtual instruments (VI) created with the use of LabVIEW.

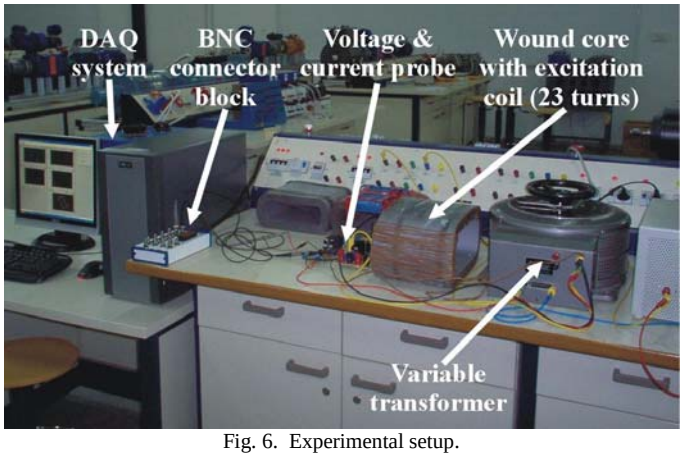

Fig. 6. Experimental setup.

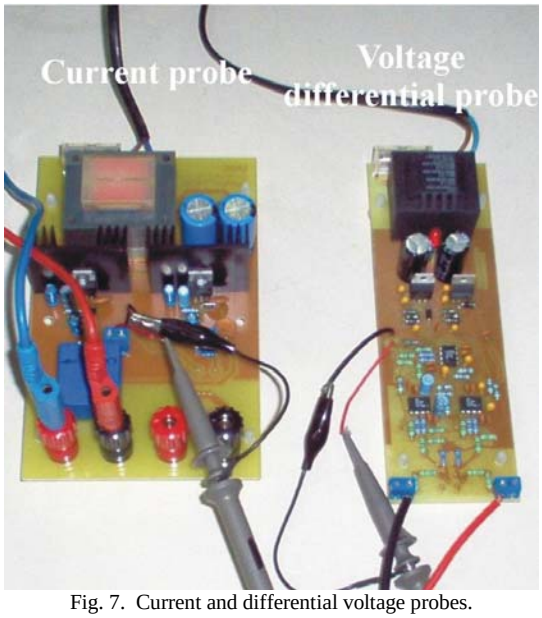

Fig. 7. Current and differential voltage probes.

Two turn search coils wound around the core's sheets, were employed for determining the peak flux distribution along the core's limb and corner for different magnetization levels. The voltages induced in the search coils were measured by connecting their terminals directly to the DAQ card's voltage differential inputs. The local peak flux density B_p is given by (22) where $\langle V \rangle$ is the average rectified voltage, f is the frequency, N is the number of turns of the search coils, and S is the cross-section area of a single steel sheet.

$$B_p = \frac{\langle V \rangle}{4fNS} \tag{22}$$

Fig. 8 illustrates a perspective view of the geometry, and the flux density vector plot of a wound core, obtained by the 3D FEM anisotropy model. The 3D FE mesh consists of 8,516 nodes and 38,798 tetrahedral elements. The core is built of high permeability magnetic steel, and the mean flux density used for the FE analysis is 1.57 T. Figs. 9 and 10 display the flux density vector and nodal plot respectively, of the upper front part of the same wound core, for a mean flux density of 1.66 T.

The computed flux density distribution across the core's limb, line AB of Fig. 8, and corner, line CD of Fig. 8, for two different magnetization levels, 1.57 T and 1.66 T, are compared with the measured ones in Figs. 11 to 14. The experimentally defined curves show that the peak flux density distribution along the limb is different from the peak flux density distribution along the corner. In both cases the peak flux density is low at the most inner steel sheets, and then it increases. However the gradient of the peak flux density is much steeper in the case of the flux density distribution across line AB.

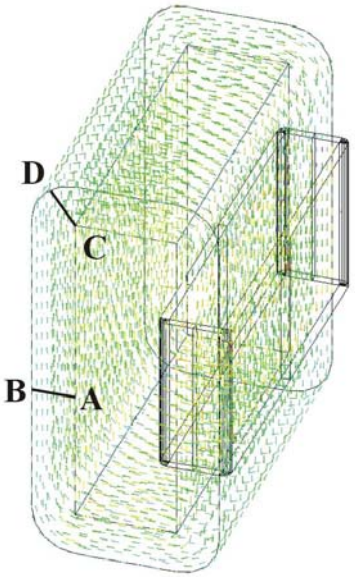

Fig. 8. Perspective view of the geometry and the peak flux density vector plot of a one-phase wound core (B = 1.57 T).

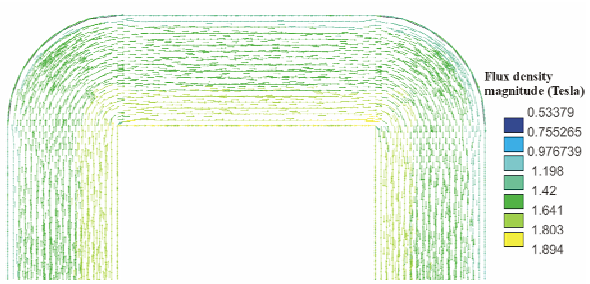

Fig. 9. Vector plot of the wound core peak flux density distribution during no load test (B = 1.66 T).

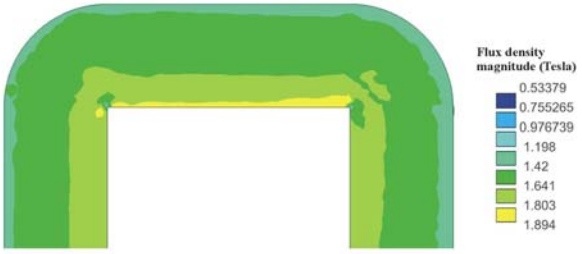

Fig. 10. Nodal plot of the wound core peak flux density distribution during no load test (B = 1.66 T).

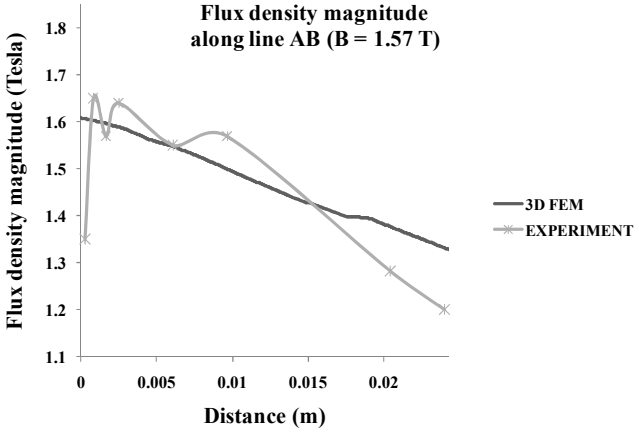

Fig. 11. Comparison of computed and measured peak flux density distribution along line AB (B = 1.57 T).

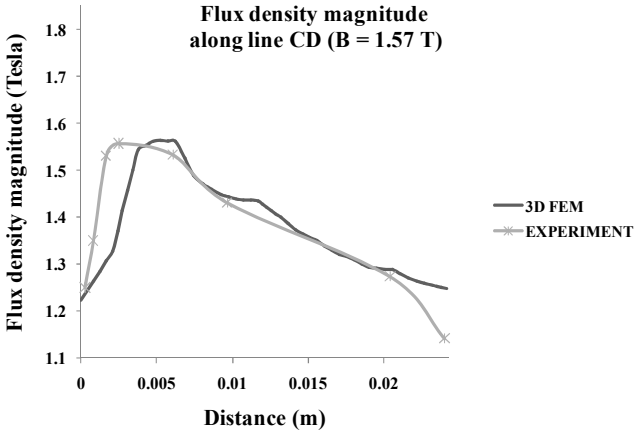

Fig. 12. Comparison of computed and measured peak flux density distribution along line CD (B = 1.57 T).

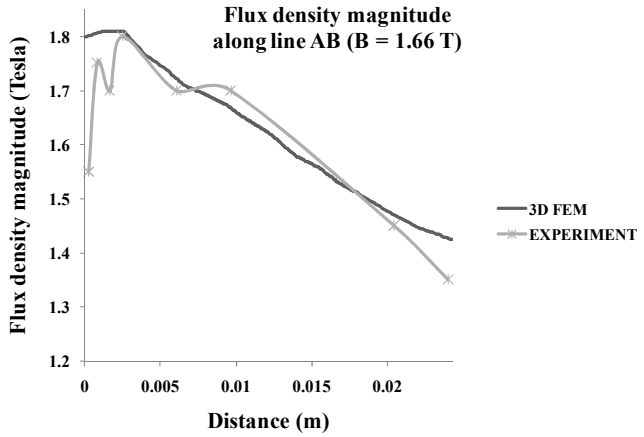

Fig. 13. Comparison of computed and measured peak flux density distribution along line AB (B = 1.66 T).

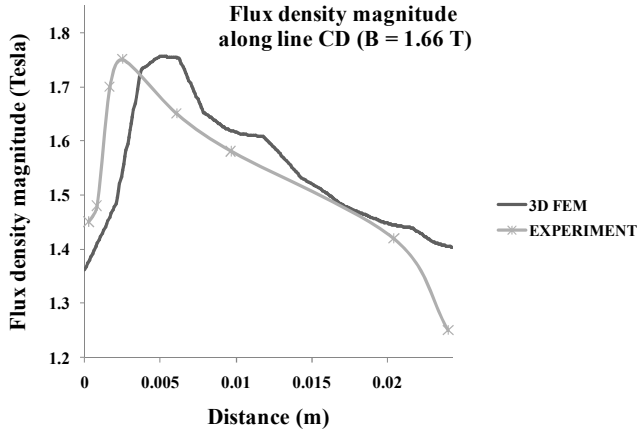

Fig. 14. Comparison of computed and measured peak flux density distribution along line CD (B = 1.66 T).

The error between calculated and measured no load loss, for a number of one-phase wound cores, was most of the times underestimated and less than 5 %. However this is not the case for the three-phase wound core transformer where the evaluation of the no load loss calls for multiple magnetostatic analysis. Table I summarizes the computed and measured no load loss of three-phase transformers of different apparent power and working induction ratings.

TABLE I
COMPARISON OF COMPUTED AND CALCULATED NO LOAD LOSS OF THREE-PHASE WOUND CORE DISTRIBUTION TRANSFORMERS

Apparent power (kVA)	Mean flux density (T)	Computed no load loss (W)	Measured no load loss (W)	Error (%)
400	1.35	553	568	2.64
630	1.37	790	830	4.82
1,600	1.55	1,642	1,620	-1.36
250	1.66	446	430	-3.72
1,000	1.72	1,277	1,350	5.41
630	1.75	1,099	1,130	2.74

The error between computed and measured no load loss is underestimated and also overestimated in some cases, whereas the error exceeds in one case 5 %.

V. CONCLUSION

The proposed 3D FE model, exhibits two important advantages when compared to conventional numerical techniques based on common potential formulations: (a) simplicity as it is based on a one-step procedure, and (b) significant computational efficiency comparing to FE methods based on standard vector and scalar potential formulations. Furthermore, the usual anisotropy models appearing at the literature are suitable mainly for modeling the core material of stack core transformers. The wound core transformer however, differs significantly from the stack core transformer and the specific anisotropy models are not suitable for the representation of laminated wound cores. In the present paper a simple and computationally effective anisotropy model was developed, appropriate specifically for the modeling of laminated wound cores.

ACKNOWLEDGMENT

This paper is part of the 03ED45 research project, implemented within the framework of the "Reinforcement Programme of Human Research Manpower" (PENED) and co-financed by National and Community Funds (25% from the Greek Ministry of Development-General Secretariat of Research and Technology and 75% from E.U.-European Social Fund).

REFERENCES

[1] W. Grimmond, A. Moses, P. Ling, "Geometrical factors affecting magnetic properties of wound toroidal cores," *IEEE Trans. Magnetics*, vol. 25, no. 3, pp. 2686-2693, May 1989.

[2] A. Basak, C. Yu, G. Lloyd, "Core loss computation of a 1000 kVA distribution transformer," *Journal of Magnetism and Magnetic Materials*, vol. 133, pp. 564-567, 1994.

[3] S. Zurek, F. Al-Naemi, A. J. Moses, "Finite-element modeling and measurements of flux and eddy current distribution in toroidal cores wound from electrical steel," *IEEE Trans. Magnetics*, vol. 44, no 6, pp. 902-905, Jun. 2008.

[4] T. Kefalas, M. Tsili, A. Kladas, "Unification of anisotropy and FEM-BE models for distribution transformer optimization," *Journal of Optoelectronics and Advanced Materials*, vol. 10, no. 5, pp. 1143-1148, May 2008.

[5] T. D. Kefalas, P. S. Georgilakis, A. G. Kladas, A. T. Souflaris, D. G. Paparigas, "Multiple grade lamination wound core: A novel technique for transformer iron loss minimization using simulated annealing with restarts and an anisotropy model," *IEEE Trans. Magnetics*, vol. 44, no 6, pp. 1082-1085, Jun. 2008.

[6] A. G. Kladas, J. A. Tegopoulos, "A new scalar potential formulation for 3D magnetostatics necessitating no source field calculation," *IEEE Trans. Magnetics*, vol. 28, no. 2, pp. 1103-1106, Mar. 1992.

[7] M. Gyimesi, J. D. Lavers, "Generalized potential formulation for 3-D magnetostatic problems," *IEEE Trans. Magnetics*, vol. 28, no. 4, pp. 1924-1929, Jul. 1992.

[8] M. Gyimesi, D. Lavers, T. Pawlak, D. Ostergaard, "Application of the general potential formulation," *IEEE Trans. Magnetics*, vol. 29, no. 2, pp. 1345-1347, Mar. 1993.

[9] H. V. Sande, T. Boonen, I. Podoleanu, F. Henrotte, K. Hameyer, "Simulation of a three-phase transformer using an improved anisotropy model," *IEEE Trans. Magnetics*, vol. 40, no. 2, pp. 850-855, Mar. 2004.